Biocatalysis and Agricultural Biotechnology 27 (2020) 101683

Contents lists available at ScienceDirect

Biocatalysis and Agricultural Biotechnology

journal homepage: http://www.elsevier.com/locate/bab

Rapid mycosynthesis and characterization of phenols-capped crystal gold nanoparticles from *Ganoderma applanatum,* Ganodermataceae

Shimal Younis Abdul-Hadi [a], Mustafa Nadhim Owaid [b,c,*], Muwafaq Ayesh Rabeea [d], Azlan Abdul Aziz [e], Mahmood S. Jameel [e]

[a] Department of Biology, College of Education for Pure Science, University of Mosul, Mosul, Iraq
[b] Department of Heet Education, General Directorate of Education in Anbar, Ministry of Education, Hit, 31007, Anbar, Iraq
[c] Department of Environmental Sciences, College of Applied Sciences-Hit, University of Anbar, Hit, 31007, Anbar, Iraq
[d] Department of Applied Chemistry, College of Applied Sciences-Hit, University of Anbar, Hit, 31007, Anbar, Iraq
[e] Nano-Optoelectronics Research and Technology Lab (NORLab), School of Physics, Universiti Sains Malaysia, 11800, Pulau Pinang, Malaysia

ARTICLE INFO

Keywords:
AuNPs
Ganoderma applanatum
Methylene blue
Nanotechnology
Reishi mushroom

ABSTRACT

This study aims to mycosynthesize crystal gold nanoparticles (AuNPs) using phenolic compounds isolated from *Ganoderma applanatum* (Reishi mushroom). The phenols-capped AuNPs were described by change of color, UV–Vis, FTIR, AFM, FESEM, TEM, HRTEM, SAED, EDX, XRD and Zeta Potential analyses. HPLC and FTIR analyses exhibited the presence of some phenolic compounds including rutin, qurcetine, epigene, keampherol, and gallic acid. The mycosynthesized AuNPs were capped by phenols as a reducer and stabilizer agent as in FTIR, and Zeta Potential. The lambda max of UV–Vis (550 nm) and EDX results proved the formation of AuNPs after 10 min. AFM, FESEM, TEM, HRTEM, and SAED images showed face-centered cubic crystals (phenols-capped AuNPs) with average 18.70 nm. The mycosynthesized phenols-capped AuNPs exhibited rapid catalytic reduction of methylene blue dye to leucomethylene blue in the existence of $NaBH_4$. This study is considered first attempt to mycosynthsize of AuNPs using phenols isolated from edible mushrooms which showed significant rapid role to decolorize MB dye.

1. Introduction

The process of formation of Au nanoparticles from biological materials is considered a modern science that comes within the green chemistry. These biological sources include seaweeds (Narendrakumar et al., 2020), medicinal plants (Chandra et al., 2020), (Seetharaman et al., 2017), bacteria (Jafari et al., 2018), and mushrooms (Rabeea et al., 2020). Besides, gold nanoparticles have miscellaneous biomedical applications (Dheyab et al., 2020).

The natural resources have been depleted due to the lack of appropriate treatment of industrial waste, especially dyes of industrial fabrics, and this poses a serious threat to the environment because of the toxicity of dyes, which is difficult to analyse (Nandhini et al., 2019). The traditional methods for removing dyes in the water are not effective. However, enzymes of basidiomycetes (Cardoso et al., 2018), Actinomycetes (Saipreethi and Manian, 2019), bacteria and some agricultural wastes (Nallapan Maniyam et al., 2020) are capable to decolorize MB. but the nanoparticles made with biological methods have been important in treating wastewater, treatments, etc. Moreover, other metallic nanoparticles synthesized from plants exhibited remarkable role to decolorize Azo dyes like methylene blue (Anchan et al., 2019; Ganesh et al., 2019).

Recently, the mycosynthesized AuNPs from mushrooms have been revealed anticancer, antioxidant and catalytic activity (Owaid and Ibraheem, 2017). Indeed, using mushrooms in the mycosynthesis of metallic nanoparticles is too important (Owaid, 2019) because of the huge amounts of fruiting bodies, mycelia and their metabolites which reduce costs and increase eco-friendly aspects (Owaid and Ibraheem, 2017).

Only few studies were achieved to reduce gold ions using isolated fungal compounds from mushrooms like glucan (polysaccharide) from *Pleurotus florida* (Sen et al., 2013), laccase (protein) from *Pleurotus ostreatus* (El-Batal et al., 2015) and Schizophyllan from *Schizophyllum commune* (Bae et al., 2007). But most of publications in this field used crude extracts of mushrooms both mycelia and fruiting bodies to synthesize AuNPs (Owaid and Ibraheem, 2017), such as *Volvariella volvacea*

* Corresponding author. Department of Heet Education, General Directorate of Education in Anbar, Ministry of Education, Hit, 31007, Anbar, Iraq.
E-mail addresses: mustafanowaid@gmail.com, mustafanowaid@uoanbar.edu.iq (M.N. Owaid).

https://doi.org/10.1016/j.bcab.2020.101683
Received 29 March 2020; Received in revised form 11 May 2020; Accepted 6 June 2020
Available online 8 June 2020
1878-8181/

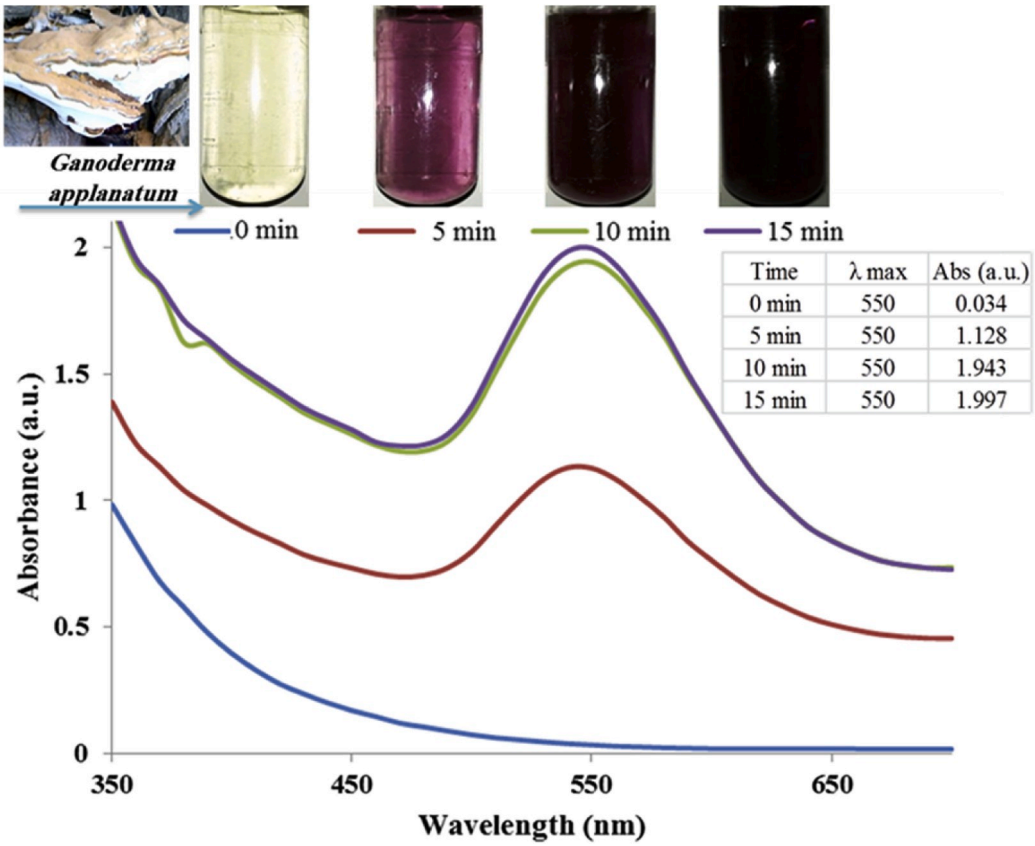

Fig. 1. UV–Vis and optical vision of the phenols-capped AuNPs.

(Philip, 2009), *Pleurotus florida* (Bhat et al., 2013), *Pleurotus sapidus* (Sarkar et al., 2013), *Grifola frondosa* (Vetchinkina et al., 2013), *Hericium erinaceus* (Raman et al., 2015), *Pleurotus cornucopiae* var. *citrinopileatus* (Owaid et al., 2017), *Flammulina velutipes* (Narayanan et al., 2015; Rabeea et al., 2020), *Agaricus bisporus* (Eskandari-Nojedehi et al., 2018; Eskandari-Nojehdehi et al., 2016), and *Lentinula edodes* (Owaid et al., 2019).

Moreover, silver nanoparticles were prepared from *Ganoderma lucidum* (Aygün et al., 2020), *Ganoderma neo-japonicum* (Gurunathan et al., 2013), *Ganoderma sessiliforme* (Mohanta et al., 2018), *Ganoderma applanatum* (Dandapat et al., 2019; Jogaiah et al., 2019). But only the species of *Ganoderma lucidum* was used to synthesize intracellular (Vetchinkina et al., 2013) and extracellular AuNPs (Kumar et al., 2017). The literature review showed that the researches referred using extracts of fruiting bodies of mushrooms more than the isolated organic compounds from them in the synthesis metallic nanoparticles (Owaid and Ibraheem, 2017). Hence, for the first time, the phenolic compounds isolated from mushrooms (exactly from *Ganoderma applanatum*) were used to synthesize the phenols-capped AuNPs in this study and applied to decolorize Methylene blue rapidly.

2. Materials and methods

2.1. Chemicals

Chloroauric acid ($HAuCl_4{\cdot}4H_2O$, purity 99.9%) was purchased from DIREVO Industrial Biotechnology (Germany). The organic solutions, including chloroform ($CHCl_3$, purity 99.5%) was obtained from Gainland Chemical Co. (England), and butanol (C_4H_9OH, purity 99%) purchased from BDH (England).

2.2. Mushroom samples

The mushroom samples were collected from Mosul city, Iraq on the *Morus* spp. tree (Moraceae) and identified as *Ganoderma applanatum* according to the morphology and microscopy characteristics (Niemelä and Miettinen, 2008). The samples of mushroom were placed on a clean place at 40 °C to dry until constant of weight. The dried samples of mushroom were milled to isolate simple phenols and polyphenols which will use in the synthesis of gold nanoparticles.

2.3. Extraction of mushroom samples

The first step is grinding and homogenization of the fruiting bodies. The extraction of the powder was achieved to isolate the bioactive phytochemicals from *Ganoderma applanatum.* Additional steps were completed to remove unwanted non-phenolic and phenolic substances like fat, wax, chlorophyll and terpene. Thirty gram of the powdered mushroom was extracted by 15 ml of chloroform with continuous stirring at room temperature for 24 h. The extract was placed in an ultrasonic device for 15 min. Then 100 ml of butanol was added and then transferred to the separation funnel. The polar organic layer (butanol) was collected and transferred to the rotary evaporator device to obtain a dry extractor. The operation was repeated 3 times to obtain an adequate amount prior to analysis (Mradu et al., 2012). The phenols dissolved in water was used in the synthesis of gold nanoparticles.

2.4. HPLC condition for analyzed phenolic compounds

The sample was analyzed using HPLC (high performance liquid chromatography) model (SYKAM) Germany. Pump model: S 2100 Quaternary Gradient Pump, Auto sampler model: S 5200, Detector: UV (S 2340) and Column Oven model: S 4115. The mobile phase was A at

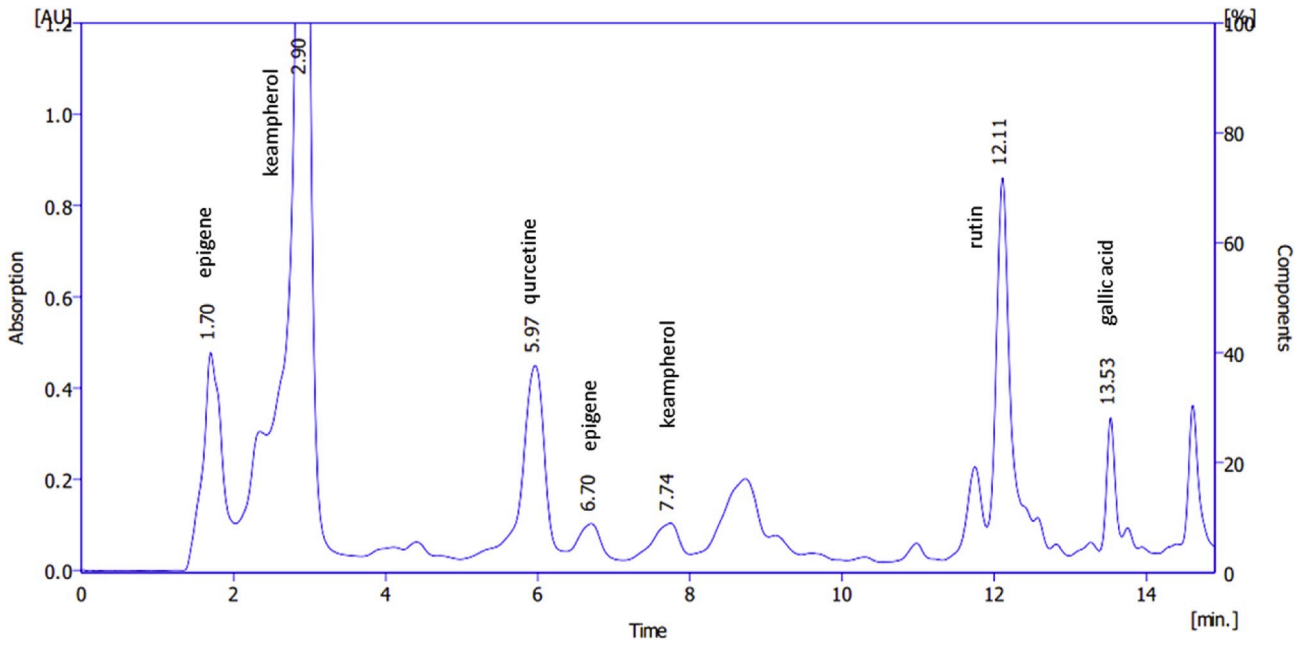

Fig. 2. HPLC of the phenolic compounds isolated from *Ganoderma applanatum*.

ratio 85:13:2 and B at ratio B 25:70:5 (Methanol:distilled water:acetic acid). The column is C18-ODS (25 cm × 4.6 mm) and detector UV–360 nm at flow rate 1 ml/min.

2.5. Green synthesis of phenols-capped AuNPs

To synthesize the phenols-capped AuNPs, 2 ml of the watery phenol solution of *Ganoderma applanatum* was added to 50 ml of chloroauric acid solution (1 mM) and placed the magnetic stirrer at 80 °C for 15 min until constancy of color and lambda max of the absorbance of the colloidal suspension AuNPs.

2.6. Characterization of the phenols-capped AuNPs

The mycosynthesized phenols-capped gold nanoparticles using *Ganoderma applanatum* were described using the change of color, UV–Visible (EMCLAB UV/VIS Spectrophotometer, Germany, Model EMC-11S–V, 325–1000 nm), FTIR (Fourier transform infrared spectroscopy) (FT7600 Lambda FT-IR Spectrometer), XRD (X-ray Diffraction) (PANalytical X'pert PRO MRD PW 3040), Zeta Potential (Nanoseries Model ZEN 3600, Malvern Instruments), SEM (scanning electron microscopy), EDX (Energy-dispersive X-ray spectroscopy) (OXFORD INSTRUMENTS X-MAX), FESEM (Field emission scanning electron microscopy) (FESEM-FEI/Nova NanoSEM 450), the selected area electron diffraction (SAED) and HRTEM (High-resolution transmission electron microscopy) (FEI, TECNAI G^2 200.000 KV). All these tests were completed in Malaysia at Universiti Sains Malaysia (USM).

2.7. Decolorization efficiency of MB by the phenols-capped AuNPs

The phenols-capped AuNPs was used to decolorize MB at room temperature. However, 1 ml of 50 mM $NaBH_4$ was mixed with 3 ml of MB dye (10 ppm) for this purpose, then 50 µl of phenols-capped AuNPs was added at room temprature. The absorbance was checked using UV–visible from 400 to 900 nm and the value at 665 nm was used to know the decolorization efficiency of this dye as the following equation (Fan et al., 2009):

$$\text{Decolorization efficiency} = (1 - At/A0) * 100 \quad (1)$$

Where, A0: the absorbance at 0 s, At: the absorbance after the incubation time (sec).

3. Results and discussion

The intensity of phenols-capped AuNPs (gold nanoparticles) increased with increasing time of incubation as in Fig. 1. The lambda max was constant recorded 550 nm while the intensity of colloidal AuNPs increased from 0.034 a.u. to 1.128 a.u. after 5 min from starting the interaction then to 1.943 a.u. and 1.997 a.u. (approx. 2.000 a.u.) after 10 and 15 min, respectively. The visual color of interaction solution changed from yellow to light purple after 5 min then the intensity increased to purple and dark purple after 10 and 15 min, respectively because increasing the AuNPs formed by phenols of *Ganoderma applanatum* in this study. The reason of the change of color to purple with the lambda max of 550 nm relates with the phenomena of surface Plasmon resonance (Owaid et al., 2019). The increasing of the interaction time led to increase the intensity of the colloidal phenols-capped AuNPs which mean more AuNPs formed because of the increased activation energy (Dutta et al., 2016).

The results of HPLC analysis of the isolated phenolic compounds from the extract of *Ganoderma applanatum* (Fig. 2) exhibited the presence of some phenolic compounds including rutin with a retention time (RT) of 12.11 min and the concentration of 5 ppm, qurcetine (RT of 5.97 min and concentration of 7.5 ppm), epigene (RT of 1.70 and 6.70 min and concentration of 10 ppm), keampherol (RT of 2.90 and 7.74 min and concentration of 15 ppm), and gallic acid (RT of 13.53 min and concentration of 15 ppm).

Phenolic compounds have the OH group directly related to the aromatic rings. In present study, Fig. 3a showed stretching vibration at the region of 1470 cm^{-1} due to C═C group in ring aromatic compounds. A deformation interaction of OH, C–O and C–O–H of phenolic compounds can corresponding stretching vibrations bands at regions ranged from 1030 to 1100 cm^{-1}, and 1320 cm^{-1}, respectively (Solimani, 1997). The carbonyl band in the carboxylic acid shifted to 1590 cm^{-1} due to the resonance effect in the aromatic ring. In addition to a very broad band of a hydroxyl group at 2941-3500 cm^{-1} overlapped with Sp^3 stretch vibration related to phenolic and carboxylic acid (Gallic acid) (Fig. 3a).

From Fig. 3a, a stretch band of the carbonyl group at 1640 cm^{-1} and the stretch band at 3400 cm^{-1} demonstrated the stability of the carboxylic acid during the preparation of AuNPs. While the disappearance

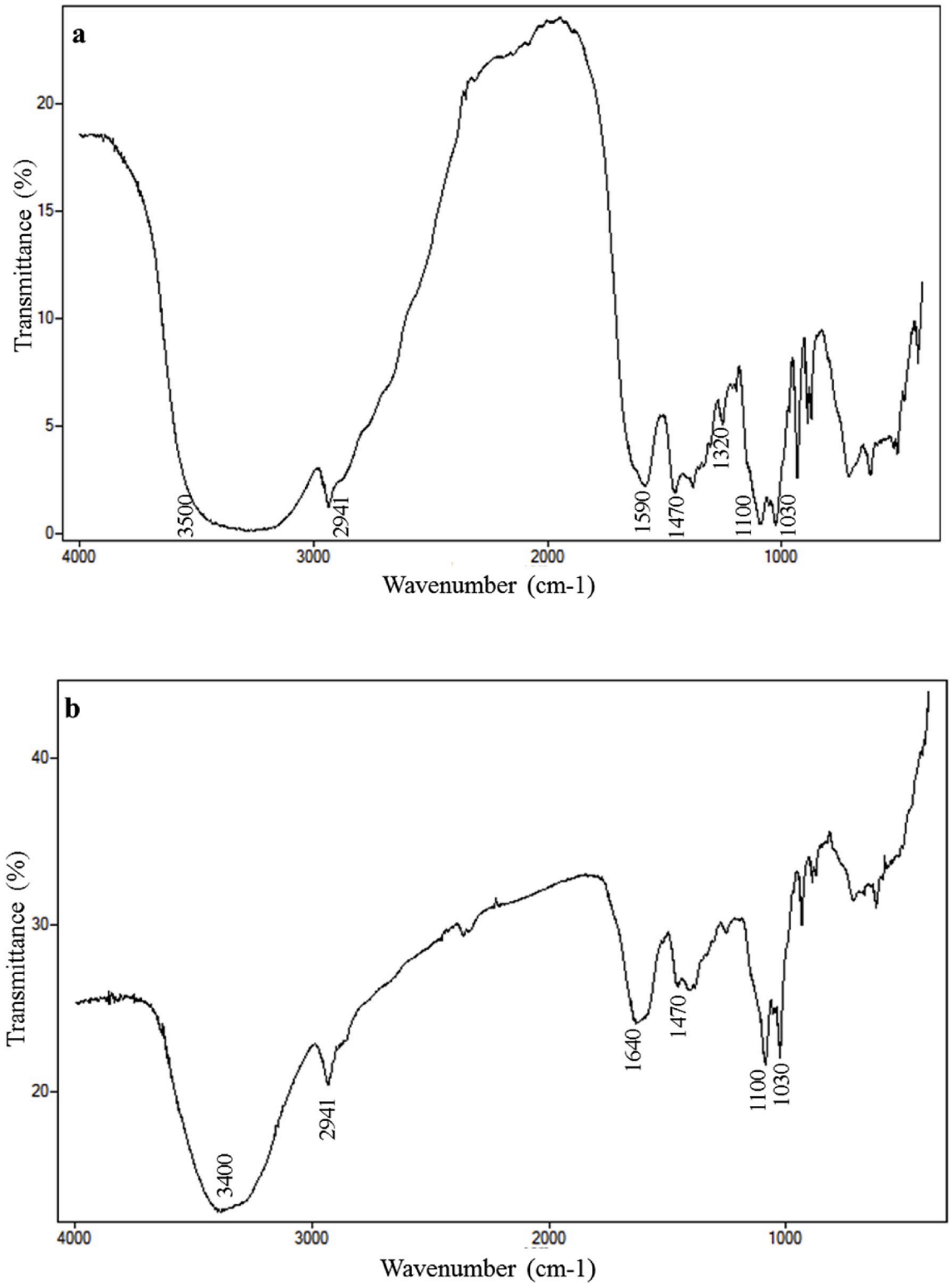

Fig. 3. FTIR of the phenolic compounds isolated from *Ganoderma applanatum* (a) the mycosynthesized AuNPs (b).

of the phenol broadband at 3500 cm^{-1} proved its association with reducing Au^{+} to Au^{0}.

Atomic force electron microscope (AFM) of the phenols-capped AuNPs synthesized from *Ganoderma applanatum* was illustrated the morphology and roughness in the 2D and 3D topographical graphics (Fig. 4). Also, this figure declared the formation of clear geometrical shapes in the gold NPs layer. This analysis was confirmed by XRD (Fig. 5), SEM, FESEM, HRTEM and SAED (Fig. 6) to know the shape, size and nature of crystalline.

Peaks of XRD in Fig. 5 positioned at 2θ of 38.20°, 44.46°, 64.58° and 77.52° could be related to crystallographic planes (1 1 1), (2 0 0), (2 2 0), and (3 1 1), respectively of face-centered cubic (fcc) Au crystals which agreed with (Eskandari-Nojedehi et al., 2018), and corresponds with Reference Code 03-065-2870 values (Herrero-Calvillo et al., 2020;

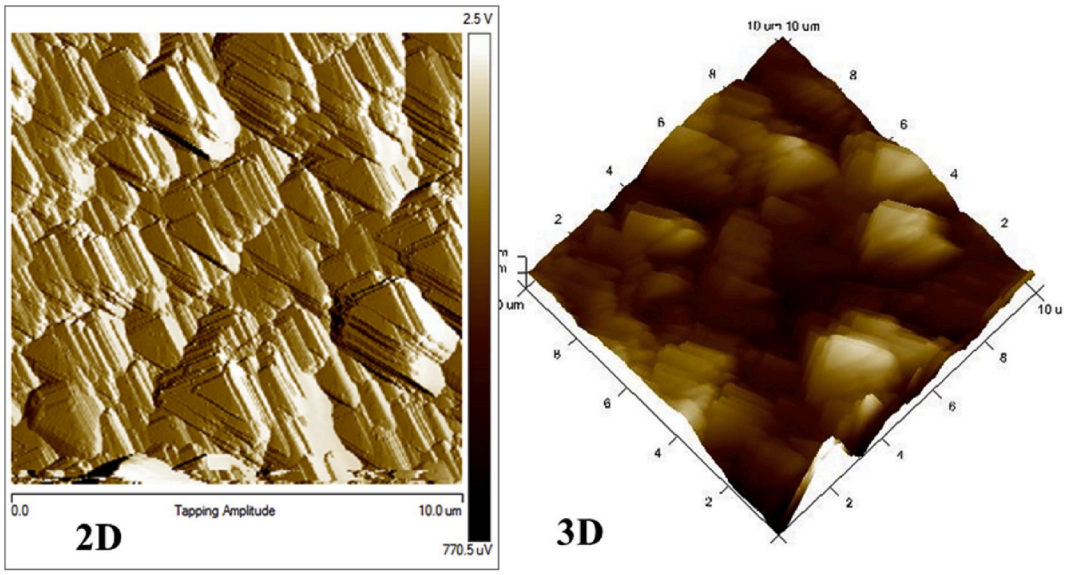

Fig. 4. AFM of the phenols-capped AuNPs synthesized from *Ganoderma applanatum*.

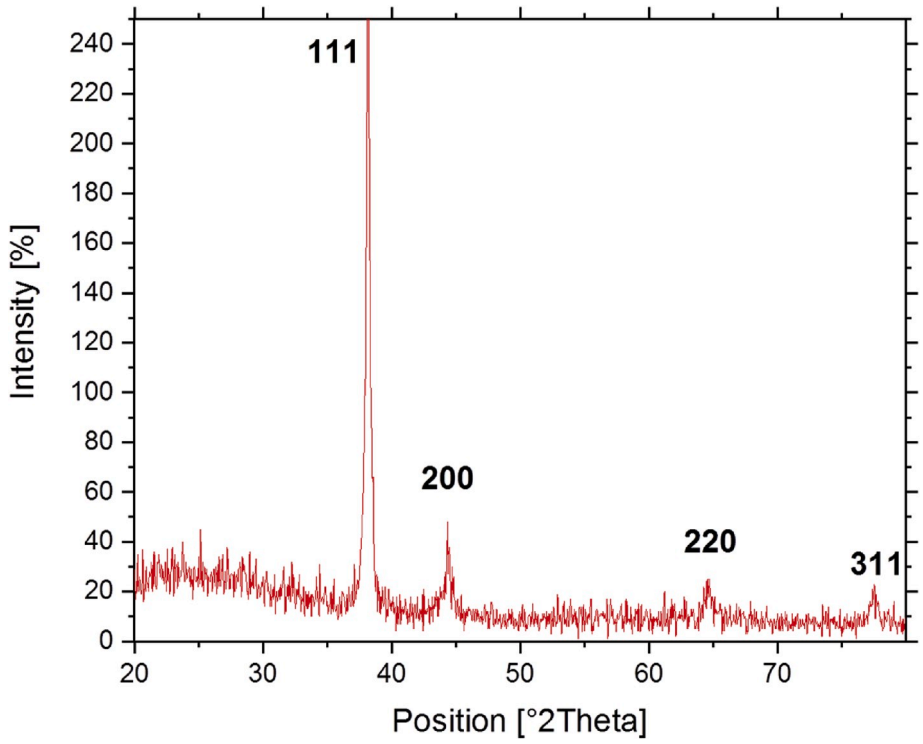

Fig. 5. XRD of the phenols-capped AuNPs.

Kumar et al., 2020). The particle size averages of grains are 35.72, 11.40, 12.48 and 14.79 nm respectively. Also, the average of size of the phenols-capped AuNPs is 18.70 nm. The peak of (1 1 1) has the highest intensity of 100%, pointing out that the current peak is a noticeable orientation, which exhibits the mean crystallite size of the phenols-capped AuNPs is 35.72 nm. The XRD pattern clearly exhibited that phenols-capped AuNPs had a crystalline nature and performed to confirm the monocrystalline. Other microstructural parameters of the phenols-capped AuNPs were listed in Table 1. The average of grains size of AuNPs was calculated using the X-ray diffraction peak through Debye–Scherrer equation (Abdelrahim et al., 2017):

$$D = 0.89\ \lambda/\beta \cos\theta \quad (2)$$

Where D is the average thickness of crystalline grain vertically at the plane of a crystal (nm), K is equal 0.89 (Scherrer constant), θ is the diffraction angle, β is FWHM (Full-Width Half Maximum (FWHM), and λ (lambda) is the X-ray wavelength (CuKα source) of 0.154 nm.

While, the dislocation density (δ) was calculated by Eq. (3) (Karthik et al., 2020):

$$\delta = (1/D^2) \ldots \ldots \quad (3)$$

SEM (Fig. 6a) and FESEM (Fig. 6b) images showed different shapes of phenols-capped AuNPs. For additional analysis of the atomic structures, HRTEM (high resolution TEM) images and SAED (selected area electron diffraction) patterns (Fig. 6) were carried out. Patterns of SAED of

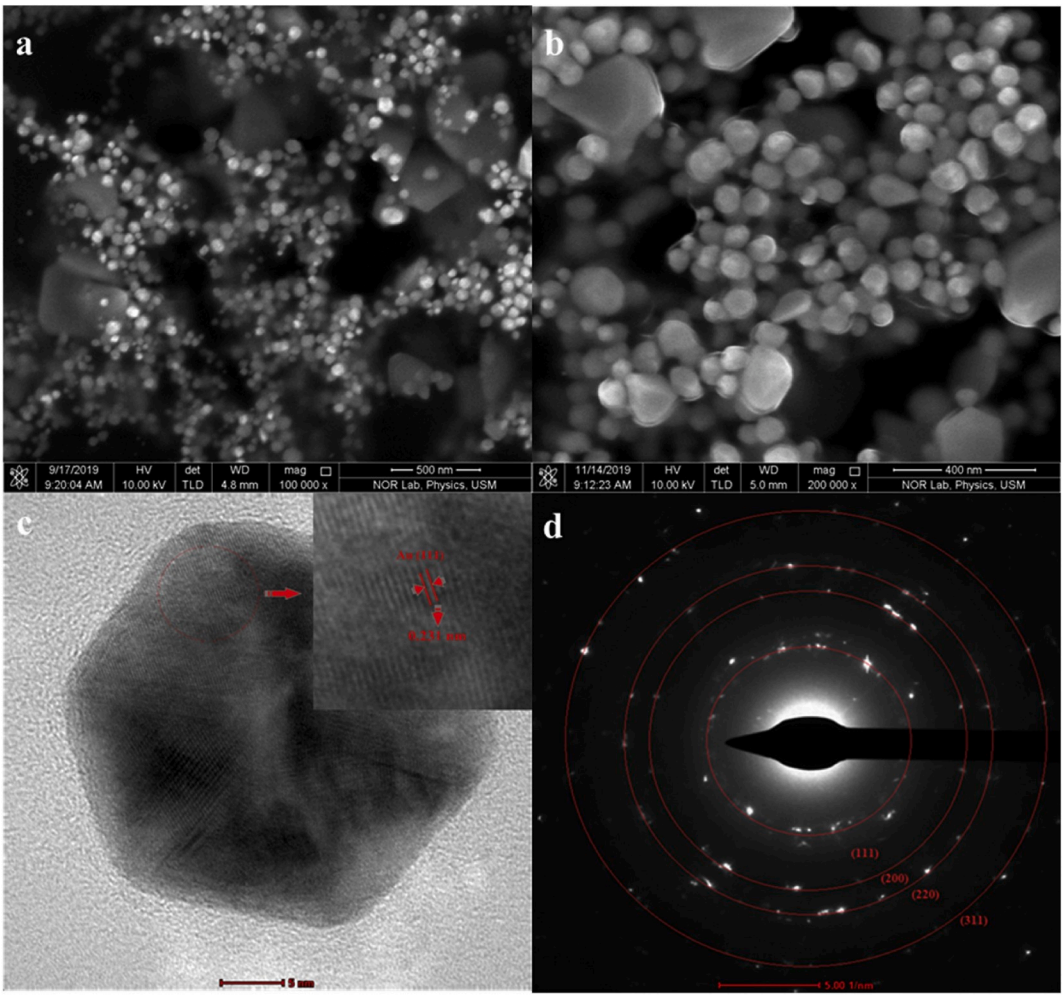

Fig. 6. Electron microscopes images for the phenols-capped AuNPs mycosynthesized from *Ganoderma applanatum* including SEM (a), FESEM (b), HRTEM (c), SAED (d).

Table 1
Microstructral parameters of the phenols-capped AuNPs.

Planes	2θ	Lattice parameter (a) (Å)	Dislocation density (δ) ($\times 10^{15}$ lines/m^2)	Crystallite Size (D) (nm)	FWHM (β)	d-spacing (Å)
1 1 1	38.20°	4.05	0.7837	35.72	0.2460	2.35574
2 0 0	44.46°	5.49	7.6947	11.40	0.7872	2.03775
2 2 0	64.58°	5.48	6.4205	12.48	0.7872	1.44303
3 1 1	77.52°	4.03	4.5716	14.79	0.7200	1.23027

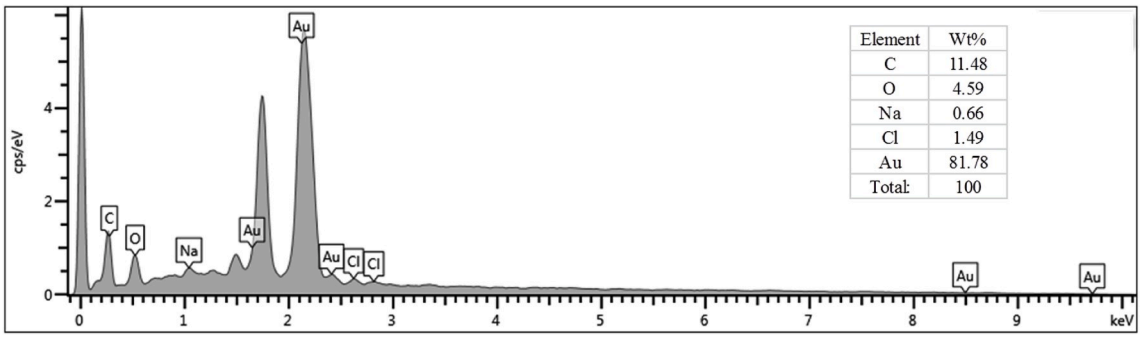

Fig. 7. EDX of the phenols-capped AuNPs.

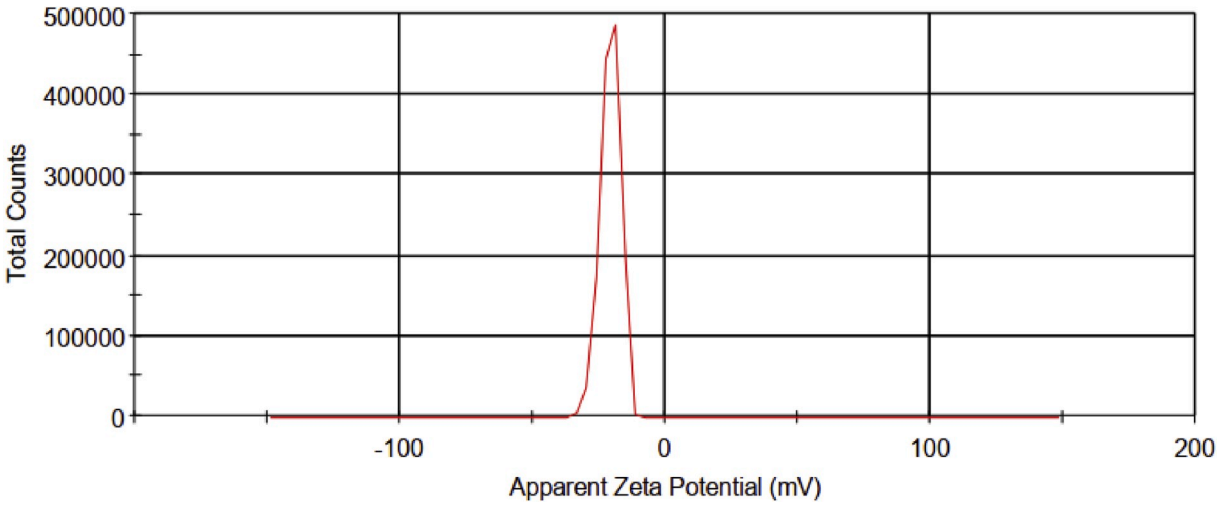

Fig. 8. Zeta Potential of the phenols-capped AuNPs.

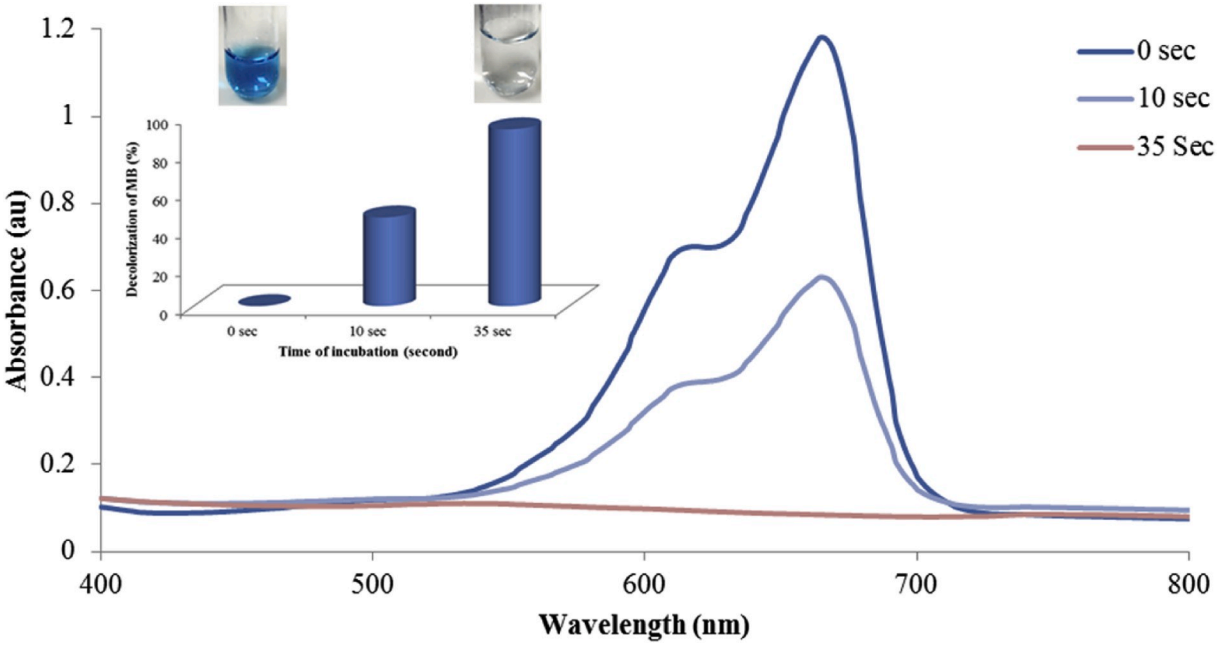

Fig. 9. Decolorization efficacy of Methylene Blue by the phenols-capped gold NPs

AuNPs are exhibited in Fig. 6d. We identified that intense circular pattern rings. This could be reflection from lattice planes of crystalline Au nanoparticles. The pattern of SAED showed the existence of bright spots with their crystal orientations appearing within the diffraction rings is an excellent confirmation of crystalline nature of the colloidal Au nanoparticles. The diameter of SAED pattern was compatible with the d-spacing and coincided with the phase of FCC of the colloidal Au nanoparticles (Khatoon et al., 2018). Also, parameters of XRD (Fig. 4) were supported SAED pattern results. However, the atomic lattice fringes of mycosynthesized AuNPs by phenols isolated from *Ganoderma applanatum* as reducing agents were noticed to be 0.231 nm as exhibited in Fig. 6d, which is closely similar to the formal value of phenols-capped AuNPs and compatible with planes of the fcc Au crystal, which informed recently (Qi et al., 2016).

The EDX image of the phenols-capped AuNPs (Fig. 7) showed the Au element at 2.15 KeV and a weight of 81.78% as an indicator for the formation of AuNPs from the phenolic compounds of *Ganoderma applanatum*. The two elements (weight of 11.48%) and Oxygen (weight of 4.59%) showed an indicator for the presence of organic compounds which isolated from this mushroom like the phenolic compounds (Khoddami et al., 2013). Whereas weaker signals from Cl (1.49%) and Na (0.66%) signals are likely to be due to X-ray emission from the solvents and the extract (Soni and Prakash, 2012) during the purification process.

The stability of the mycosynthesized phenols-capped AuNPs was investigated using zeta potential analysis. Fig. 8 exhibited the surface zeta potential, which showed the surface charge on phenols-capped gold NPs. Also, the zeta potential value revealed the constancy of these nanoparticles (Srikar et al., 2016). Hence, biosynthesized gold NPs had a promising zeta potential value of -20.6 ± 3.76 mV formed from the phenolic compounds of *Ganoderma applanatum*. Nevertheless, the zeta potential value referred to good quality with weak aggregation of gold NPs (Suresh et al., 2011).

Moreover, the negative value of this test signed to that AuNPs were surrounded by negatively charged phenolic compounds as a reducing and capping agent led to increase the stability of the formed phenols-

Table 2
Results of the current study compared to the previously published related literature.

Mushrooms	NPs Type (concentration)	Sizes and shapes of NPs	Conditions and time	Using $NaBH_4$	The dye type and the concentration	Decolorization percentages of MB	References
Flammulina velutipes Fruitbodies	AuNP (5 mg)	74 nm (triangular, spherical, and irregular)	25 °C with shaking (240 min)	No	20 ppm Methylene Blue	75%	Rabeea et al. (2020)
Ganoderma lucidum Fruitbodies	AgNP (10 mg)	10–80 nm (Rod, and needle-like)	UV irradiation 265 nm (150 min)	No	10 ppm Direct blue 71	78–97%	Sriramulu and Sumathi (2017)
Agaricus bisporus sFruitbodies	AgNP (10 mg)	10–80 nm (Sponge-like)	UV irradiation 265 nm (150 min)	No	10 ppm Direct blue 71	93–96%	Sriramulu and Sumathi (2017)
Ganoderma applanatum phenols	Phenols-capped AuNP (50 µl)	18.70 nm (centered cubic crystals)	at room temperature (35 s)	50 mM	10 ppm Methylene Blue	92.83%	This study

capped AuNPs. Many studies have characterized that the stabilizers (surface-active biomolecules) in reaction solutions lead to create many electrostatic interactions are giving more stable gold NPs (Ahmad et al., 2015; Anand et al., 2015). It is proposed that the phenol or flavonoid can act as a stabilizer accountable for the biosynthesis and constancy of Au nanoparticles. Finally, the metallic NP is considered to be firm if values of its potential surface is between +30 and −30mV (Anand et al., 2015).

Finally, Fig. 9 exhibited UV–Visible specta of the degradation of MB and the decolorization efficiency of The phenols-capped AuNPs. Rapidly, these AuNPs decolored the MB dye and recorded decolorization efficiency of 46.61% and 92.83% after 10 s and 35 s at room temperature, respectively. The lambda max was constant 665 nm and the absorbance reduced rapidly from 1.182 a.u. for the control at 0 s to 0.631 a.u. and 0.084 a.u. after 10 s and 35 s respectively as seen in Fig. 9. The catalytic efficiency increased with increase of the area of surface, and metallic NPs possess more surface area because of their fine sizes (Vidhu and Philip, 2014) especially with these gold nanoparticles which had size reaches 18.70 nm. Gold nanoparticles acted as a substrate for the electrotransfer reaction thus gold NPs facilitated electrons transfer from donor (BH_4^- ions) to acceptor (Methylene blue) to form leucomethylene blue (Narayanan and Park, 2015). The absorbance intensity at 665 nm in the presence MB decreased rapidly with the time, which confirmed that AuNPs act as active catalysts through the rapid reduction of Methylene blue. These characteristics cause to be metallic NPs as more helpful agents for the treatment of industrial textile dyes. Nevertheless, Table 2 showed similar catalytic activity by metallic NPs synthesized from mushrooms has been reported and some differences among this research and others which synthesized NPs from the mushroom and used for decolorizing Blue Azo dyes.

4. Conclusion

This study aims to mycosynthesize crystal gold nanoparticles (AuNPs) using phenolic compounds isolated from *Ganoderma applanatum*. The presence of rutin, qurcetine, epigene, keampherol, and gallic acid led to mycosynthsize AuNPs as a reducer and stabilizer agents. The lambda max of UV–Vis was recorded 550 nm. EDX results proved the formation of AuNPs after 10 min. AFM, FESEM, TEM, HRTEM, and SAED images showed face-centered cubic crystals (phenols-capped AuNPs) with average 18.70 nm. The mycosynthesized phenols-capped AuNPs exhibited rapid catalytic reduction of methylene blue dye to leucomethylene blue in the existence of $NaBH_4$. This study is considered first attempt to mycosynthsize of AuNPs using phenols isolated from edible mushrooms which showed significant rapid role to decolorize MB dye.

Declaration of competing interest

The authors declare that they have no known competing financial interests or personal relationships that could have appeared to influence the work reported in this paper.

Acknowledgments

The authors thank the School of Physics in USM for their support of this research via FRGS Grant No. 203.PFIZIK.6711768, to achieve some measurements of the electron microscope.

References

Abdelrahim, K., Younis, S., Mohamed, A., Salmeen, K., Mustafa, A.E.M.A., Moussa, S., 2017. Extracellular biosynthesis of silver nanoparticles using *Rhizopus stolonifer*. Saudi J. Biol. Sci. 24, 208–216. https://doi.org/10.1016/j.sjbs.2016.02.025.

Ahmad, A., Wei, Y., Syed, F., Imran, M., Khan, Z.U.H., Tahir, K., Khan, A.U., Raza, M., Khan, Q., Yuan, Q., 2015. Size dependent catalytic activities of green synthesized gold nanoparticles and electro-catalytic oxidation of catechol on gold nanoparticles modified electrode. RSC Adv. 5, 99364–99377.

Anand, K., Gengan, R.M., Phulukdaree, A., Chuturgoon, A., 2015. Agroforestry waste *Moringa oleifera* petals mediated green synthesis of gold nanoparticles and their anti-cancer and catalytic activity. J. Ind. Eng. Chem. 21, 1105–1111. https://doi.org/10.1016/j.jiec.2014.05.021.

Anchan, S., Pai, S., Sridevi, H., Varadavenkatesan, T., Vinayagam, R., Selvaraj, R., 2019. Biogenic synthesis of ferric oxide nanoparticles using the leaf extract of *Peltophorum pterocarpum* and their catalytic dye degradation potential. Biocatal. Agric. Biotechnol. 20, 101251. https://doi.org/10.1016/j.bcab.2019.101251.

Aygün, A., Özdemir, S., Gülcan, M., Cellat, K., Şen, F., 2020. Synthesis and characterization of Reishi mushroom-mediated green synthesis of silver nanoparticles for the biochemical applications. J. Pharmaceut. Biomed. Anal. 178, 112970. https://doi.org/10.1016/j.jpba.2019.112970.

Bae, A.H., Numata, M., Yamada, S., Shinkai, S., 2007. New approach to preparing one-dimensional Au nanowires utilizing a helical structure constructed by schizophyllan. New J. Chem. 31, 618–622. https://doi.org/10.1039/b615757b.

Bhat, R., Sharanabasava, V.G., Deshpande, R., Shetti, U., Sanjeev, G., Venkataraman, A., 2013. Photo-bio-synthesis of irregular shaped functionalized gold nanoparticles using edible mushroom *Pleurotus florida* and its anticancer evaluation. J. Photochem. Photobiol. B Biol. 125, 63–69. https://doi.org/10.1016/j.jphotobiol.2013.05.002.

Cardoso, B.K., Linde, G.A., Colauto, N.B., do Valle, J.S., 2018. *Panus strigellus* laccase decolorizes anthraquinone, azo, and triphenylmethane dyes. Biocatal. Agric. Biotechnol. 16, 558–563. https://doi.org/10.1016/j.bcab.2018.09.026.

Chandra, H., Kumari, P., Bontempi, E., Yadav, S., 2020. Medicinal plants: treasure trove for green synthesis of metallic nanoparticles and their biomedical applications. Biocatal. Agric. Biotechnol. 24, 101518. https://doi.org/10.1016/j.bcab.2020.101518.

Dandapat, S., Kumar, M., Ranjan, R., Sinha, M.P., 2019. Acute and sub-acute toxicity of *Ganoderma applanatum* (Pres.) Pat. Extract mediated silver nanoparticles on rat. Not. Sci. Biol. 11, 351–363. https://doi.org/10.15835/nsb11310473.

Dheyab, M.A., Abdul Aziz, A., Jameel, M.S., Noqta, O.A., Mehrdel, B., 2020. Synthesis and coating methods of biocompatible iron oxide/gold nanoparticle and nanocomposite for biomedical applications. Chin. J. Phys. 64, 305–325. https://doi.org/10.1016/j.cjph.2019.11.014.

Dutta, A., Paul, A., Chattopadhyay, A., 2016. The effect of temperature on the aggregation kinetics of partially bare gold nanoparticles. RSC Adv. 6, 82138–82149. https://doi.org/10.1039/c6ra17561a.

El-Batal, A.I., Elkenawy, N.M., Yassin, A.S., Amin, M.A., 2015. Laccase production by *Pleurotus ostreatus* and its application in synthesis of gold nanoparticles $. Biotechnol. Rep. 5, 31–39. https://doi.org/10.1016/j.btre.2014.11.001.

Eskandari-Nojedehi, M., Jafarizadeh-Malmiri, H., Rahbar-Shahrouzi, J., 2018. Hydrothermal green synthesis of gold nanoparticles using mushroom (*Agaricus bisporus*) extract: physico-chemical characteristics and antifungal activity studies. Green Process. Synth. 7, 38–47. https://doi.org/10.1515/gps-2017-0004.

Eskandari-Nojehdehi, M., Jafarizadeh-Malmiri, H., Rahbar-Shahrouzi, J., 2016. Optimization of processing parameters in green synthesis of gold nanoparticles using microwave and edible mushroom (*Agaricus bisporus*) extract and evaluation of their antibacterial activity. Nanotechnol. Rev. 5, 537–548. https://doi.org/10.1515/ntrev-2016-0064.

Fan, J., Guo, Y., Wang, J., Fan, M., 2009. Rapid decolorization of azo dye methyl orange in aqueous solution by nanoscale zerovalent iron particles. J. Hazard Mater. 166, 904–910. https://doi.org/10.1016/j.jhazmat.2008.11.091.

Ganesh, M., Lee, S.G., Jayaprakash, J., Mohankumar, M., Jang, H.T., 2019. Hydnocarpus alpina Wt extract mediated green synthesis of ZnO nanoparticle and screening of its anti-microbial, free radical scavenging, and photocatalytic activity. Biocatal. Agric. Biotechnol. 19, 101129. https://doi.org/10.1016/j.bcab.2019.101129.

Gurunathan, S., Raman, J., Abd Malek, S.N., John, P.A., Vikineswary, S., 2013. Green synthesis of silver nanoparticles using *Ganoderma neo-japonicum* Imazeki: a potential cytotoxic agent against breast cancer cells. Int. J. Nanomed. 8, 4399–4413. https://doi.org/10.2147/IJN.S51881.

Herrero-Calvillo, R., Santoveña-Uribe, A., Esparza, R., Rosas, G., 2020. A photocatalytic and electrochemical study of gold nanoparticles synthesized by a green approach. Mater. Res. Express 7, 015019. https://doi.org/10.1088/2053-1591/ab61bd.

Jafari, M., Rokhbakhsh-Zamin, F., Shakibaie, M., Moshafi, M.H., Ameri, A., Rahimi, H.R., Forootanfar, H., 2018. Cytotoxic and antibacterial activities of biologically synthesized gold nanoparticles assisted by *Micrococcus yunnanensis* strain J2. Biocatal. Agric. Biotechnol. 15, 245–253. https://doi.org/10.1016/j.bcab.2018.06.014.

Jogaiah, S., Kurjogi, M., Abdelrahman, M., Hanumanthappa, N., Tran, L.S.P., 2019. *Ganoderma applanatum*-mediated green synthesis of silver nanoparticles: structural characterization, and *in vitro* and *in vivo* biomedical and agrochemical properties. Arab. J. Chem. 12, 1108–1120. https://doi.org/10.1016/j.arabjc.2017.12.002.

Karthik, K., Pushpa, S., Naik, M.M., Vinuth, M., 2020. Influence of Sn and Mn on structural, optical and magnetic properties of spray pyrolysed CdS thin films. Mater. Res. Innovat. 24, 82–86. https://doi.org/10.1080/14328917.2019.1597436.

Khatoon, U.T., Rao, G.V.S.N., Mantravadi, K.M., Oztekin, Y., 2018. Strategies to synthesize various nanostructures of silver and their applications - a review. RSC Adv. 8, 19739–19753. https://doi.org/10.1039/c8ra00440d.

Khoddami, A., Wilkes, M.A., Roberts, T.H., 2013. Techniques for analysis of plant phenolic compounds. Molecules 18, 2328–2375. https://doi.org/10.3390/molecules18022328.

Kumar, A., Das, N., Satija, N.K., Mandrah, K., Roy, S.K., Rayavarapu, R.G., 2020. A novel approach towards synthesis and characterization of non-cytotoxic gold nanoparticles using taurine as capping agent. Nanomaterials 10, 45. https://doi.org/10.3390/nano10010045.

Kumar, D.S.R.S., Senthilkumar, P., Surendran, L., Sudhagar, B., 2017. *Ganoderma lucidum*-oriental mushroom mediated synthesis of gold nanoparticles conjugated with doxorubicin and evaluation of its anticancer potential on human breast cancer mcf-7/dox cells. Int. J. Pharm. Pharmaceut. Sci. 9, 267. https://doi.org/10.22159/ijpps.2017v9i9.20093.

Mohanta, Y.K., Nayak, D., Biswas, K., Singdevsachan, S.K., Abd_Allah, E.F., Hashem, A., Alqarawi, A.A., Yadav, D., Mohanta, T.K., 2018. Silver nanoparticles synthesized using wild mushroom show potential antimicrobial activities against food borne pathogens. Molecules 23, 1–18. https://doi.org/10.3390/molecules23030655.

Mradu, G., Saumyakanti, S., Sohini, M., Arup, M., 2012. HPLC profiles of standard phenolic compounds present in medicinal plants. Int. J. Pharmacogn. Phytochem. Res. 4, 162–167.

Nallapan Maniyam, M., Hari, M., Yaacob, N.S., 2020. Enhanced methylene blue decolourization by *Rhodococcus* strain UCC 0003 grown in banana peel agricultural waste through response surface methodology. Biocatal. Agric. Biotechnol. 23, 101486. https://doi.org/10.1016/j.bcab.2019.101486.

Nandhini, N.T., Rajeshkumar, S., Mythili, S., 2019. The possible mechanism of eco-friendly synthesized nanoparticles on hazardous dyes degradation. Biocatal. Agric. Biotechnol. 19, 101138. https://doi.org/10.1016/j.bcab.2019.101138.

Narayanan, K.B., Park, H.H., 2015. Homogeneous catalytic activity of gold nanoparticles synthesized using turnip (*Brassica rapa* L.) leaf extract in the reductive degradation of cationic azo dye. Kor. J. Chem. Eng. 32, 1273–1277. https://doi.org/10.1007/s11814-014-0321-y.

Narayanan, K.B., Park, H.H., Han, S.S., 2015. Synthesis and characterization of biomatrixed-gold nanoparticles by the mushroom *Flammulina velutipes* and its heterogeneous catalytic potential. Chemosphere 21, 169–175. https://doi.org/10.1016/j.chemosphere.2015.06.101.

Narendrakumar, V., Kumar, V.R., Karthick, V., Kumar, C.M.V., 2020. Antimicrobial effect of *Sargassum plagiophyllum* mediated gold nanoparticles on Escherichia coli and Salmonella typhi. Biocatal. Agric. Biotechnol. 101627. https://doi.org/10.1016/j.bcab.2020.101627.

Niemelä, T., Miettinen, O., 2008. The identity of *Ganoderma applanatum* (Basidiomycota). Taxon 57, 963–966. https://doi.org/10.1002/tax.573024.

Owaid, M.N., 2019. Green synthesis of silver nanoparticles by *Pleurotus* (oyster mushroom) and their bioactivity : Review. Environ. Nanotechnol. Monit. Manag. 12, 100256. https://doi.org/10.1016/j.enmm.2019.100256.

Owaid, M.N., Al-Saeedi, S.S.S., Abed, I.A., 2017. Biosynthesis of gold nanoparticles using yellow oyster mushroom *Pleurotus cornucopiae* var. *citrinopileatus*. Environ. Nanotechnol. Monit. Manag. 8, 157–162. https://doi.org/10.1016/j.enmm.2017.07.004.

Owaid, M.N., Ibraheem, I.J., 2017. Mycosynthesis of nanoparticles using edible and medicinal mushrooms. Eur. J. Nanomed. 9, 5–23. https://doi.org/10.1515/ejnm-2016-0016.

Owaid, M.N., Rabeea, M.A., Abdul Aziz, A., Jameel, M.S., Dheyab, M.A., 2019. Mushroom-assisted synthesis of triangle gold nanoparticles using the aqueous extract of fresh *Lentinula edodes* (shiitake), Omphalotaceae. Environ. Nanotechnol. Monit. Manag. 12, 100270. https://doi.org/10.1016/j.enmm.2019.100270.

Philip, D., 2009. Biosynthesis of Au, Ag and Au–Ag nanoparticles using edible mushroom extract. Spectrochim. Acta Part A Mol Biomol Spectrosc 73, 374–381. https://doi.org/10.1016/j.saa.2009.02.037.

Qi, M., Zhang, Y., Cao, C., Lu, Y., Liu, G., 2016. Increased sensitivity of extracellular glucose monitoring based on AuNP decorated GO nanocomposites. RSC Adv. 6, 39180–39187. https://doi.org/10.1039/c6ra04975c.

Rabeea, M.A., Owaid, M.N., Aziz, A.A., Jameel, M.S., Dheyab, M.A., 2020. Mycosynthesis of gold nanoparticles using the extract of *Flammulina velutipes*, Physalacriaceae, and their efficacy for decolorization of methylene blue. J. Environ. Chem. Eng. 103841. https://doi.org/10.1016/j.jece.2020.103841.

Raman, J., Lakshmanan, H., John, P., Zhijian, C., Periasamy, V., David, P., Naidu, M., Sabaratnam, V., 2015. Neurite outgrowth stimulatory effects of myco synthesized auNPs from *Hericium erinaceus* (Bull.: Fr.) Pers. on pheochromocytoma (Pc-12) cells. Int. J. Nanomed. 10, 5853–5863.

Saipreethi, P., Manian, R., 2019. Probing the biomolecular targets of azo colorant carcinogens towards purified wetland peroxidase-computational cum *in vitro* validation. Biocatal. Agric. Biotechnol. 19, 101127. https://doi.org/10.1016/j.bcab.2019.101127.

Sarkar, J., Kalyan, S., Laskar, A., Chattopadhyay, D., Acharya, K., 2013. Bioreduction of chloroaurate ions to gold nanoparticles by culture filtrate of *Pleurotus sapidus* Quel. Mater. Lett. 92, 313–316. https://doi.org/10.1016/j.matlet.2012.10.130.

Seetharaman, P., Chandrasekaran, R., Gnanasekar, S., Mani, I., Sivaperumal, S., 2017. Biogenic gold nanoparticles synthesized using *Crescentia cujete* L. and evaluation of their different biological activities. Biocatal. Agric. Biotechnol. 11, 75–82. https://doi.org/10.1016/j.bcab.2017.06.004.

Sen, I., Maity, K., Islam, S.S., 2013. Green synthesis of gold nanoparticles using a glucan of an edible mushroom and study of catalytic activity. Carbohydr. Polym. 91, 518–528. https://doi.org/10.1016/j.carbpol.2012.08.058.

Solimani, R., 1997. The flavonols quercetin, rutin and morin in DNA solution: UV-vis dichroic (and mid-infrared) analysis explain the possible association between the biopolymer and a nucleophilic vegetable-dye. Biochim. Biophys. Acta 1336, 281–294. https://doi.org/10.1016/s0304-4165(97)00038-x.

Soni, N., Prakash, S., 2012. Entomopathogenic fungus generated Nanoparticles for enhancement of efficacy in *Culex quinquefasciatus* and *Anopheles stephensi*. Asian Pac. J. Trop. Dis. 2 https://doi.org/10.1016/S2222-1808(12)60181-9, 0–5.

Srikar, S.K., Giri, D.D., Pal, D.B., Mishra, P.K., Upadhyay, S.N., 2016. Green synthesis of silver nanoparticles: a review. Green Sustain. Chem. 6, 34–56. https://doi.org/10.4236/gsc.2016.61004.

Sriramulu, M., Sumathi, S., 2017. Photocatalytic, antioxidant, antibacterial and anti-inflammatory activity of silver nanoparticles synthesised using forest and edible mushroom. Adv. Nat. Sci. Nanosci. Nanotechnol. 8, 045012 https://doi.org/10.1088/2043-6254/aa92b5.

Suresh, A.K., Doktycz, M.J., Wang, W., Moon, J.W., Gu, B., Meyer III, H.M., Hensley, D. K., Retterer, S.T., Allison, D.P., Phelps, T.J., 2011. Monodispersed Biocompatible Ag2S Nanoparticles: Facile Extracellular Bio-Fabrication Using the Gamma-Proteobacterium, S. oneidensis. Oak Ridge National Laboratory (ORNL); Center for Nanophase Materials Sciences; High Temperature Materials Laboratory.

Vetchinkina, E.P., Loshchinina, E.A., Burov, A.M., Nikitina, V.E., 2013. Bioreduction of gold (iii) ions from hydrogen tetrachloaurate to the elementary state by edible cultivated medicinal xylotrophic Basidiomycetes belonging to various systematic groups and molecular mechanisms of gold nanoparticles biological synthesis. Sci. Pract. J. Health Life Sci. 4, 51–56.

Vidhu, V.K., Philip, D., 2014. Catalytic degradation of organic dyes using biosynthesized silver nanoparticles. Micron 56, 54–62. https://doi.org/10.1016/j.micron.2013.10.006.